A PHOTOELASTIC STUDY
OF A LATERALLY LOADED PILE

A Thesis

Presented to

the Faculty of the Department of Mechanical Engineering

University of Houston

In Partial Fulfillment

of the Requirements for the Degree

Master of Science in Mechanical Engineering

by

F. Allan Bryant

January, 1969

ACKNOWLEDGMENTS

The author would like to acknowledge his indebtedness for the guidance and assistance provided by the faculty and staff of the Cullen College of Engineering especially Mr. L. J. Castellanos, Dr. C. D. Michalopoulos, Dr. W. J. Graff and Mr. A. J. Bonar.

A PHOTOELASTIC STUDY
OF A LATERALLY LOADED PILE

An Abstract of a Thesis

Presented to

the Faculty of the Department of Mechanical Engineering

University of Houston

In Partial Fulfillment

of the Requirements for the Degree

Master of Science in Mechanical Engineering

---

by

F. Allan Bryant

January, 1969

ABSTRACT

This thesis describes a test conducted to determine the feasibility of using the photoelastic method of analysis to evaluate the bending moments and deflections of a laterally loaded pile embedded in soil,

A model pile and model soil were designed and built to simulate a full scale pile and soil for which complete test data was available. The simulation procedures are described and discussed in detail. The model was tested in the polariscope and from photoelastic data the bending moments and deflections were determined. Scaling factors were applied to the full scale data to allow direct comparison with the model test results.

It was concluded that the simulation was reasonably accurate and that further photoelastic tests are justified. Also several improvements in the test procedure are suggested and discussed.

TABLE OF CONTENTS

LIST OF FIGURES

LIST OF TABLES

NOMENCLATURE

E	modulus of elasticity
E_s	soil modulus of pile reaction
E_1	modulus of beam number one
E_2	modulus of beam number two
f	material fringe value
h	pile height
I	moment of inertia
I_1	moment of inertia of beam number one
I_2	moment of inertia of beam number two
K_F	force scale factor P_1/P_2
K_L	length scale factor L_1/L_2
L_1	length of beam number one
L_2	length of beam number two
L/D	pile length to diameter ratio
M	bending moment
n	fringe order
p	maximum principal stress
P	applied force
q	minimum principal stress
t	pile thickness
W_1	weight per foot beam number one
W_2	weight per foot beam number two
x	length along pile measured from top reaction point
y	pile lateral deflection

δ linear deflection

δ_o deflection under uniform stress conditions

δ_ϵ deflection under contact stress conditions

θ Tardy angle ($\theta = 0$ for dark field)

σ bending stress

σ_3 confining pressure (triaxial test)

CHAPTER I

INTRODUCTION

The subject of this thesis is a photoelastic study of a laterally loaded pile. The problem of determining bending moments and deflections in laterally loaded piles has received considerable attention in the literature of Civil Engineering. This interest is largely due to the widespread use of piling in the offshore oil industry.

A pile is normally used to transmit a load or system of loads into the soil, and as pointed out by Ripperger (19), the problem is, in this respect, somewhat analogous to a contact stress problem. The pile problem differs, however, in two important aspects. First, soils do not normally lend themselves to analysis by the method of the theory of elasticity as do most metals; and second, piles and soils are subject to relatively large deflections thus increasing the problems associated with maintaining compatability between the stresses and strains of the soil and those of the pile.

Historically the laterally loaded pile problem has been approached in three different ways. The first significant area of investigation has been purely analytical. By this method the pile has been analyzed as a beam on an elastic support. For this condition the deflection curve for the pile is the solution of the differential equation I.

$$EI\frac{d^4y}{dx^4} = -E_s y \tag{I}$$

Where EI is the pile stiffness,
y is the lateral displacement,
x is the distance along the pile, and
E_s is the soil modulus of pile reaction.

The solution of Equation I is dependent on the nature of E_s. In 1930 Timoshenko (23) contributed the analytical solution of Equation I for the case E_s = Constant, and in 1935 Rifadt (18) solved the case of E_s a linear function of x. Palmer and Thompson (15) in 1948 solved the equation by numerical methods assuming E_s to be an exponential function of x, and in 1953 Palmer and Brown (14) used this technique to analyze the results of full scale tests. Also in 1953 Gleser (6) generalized the method of Palmer and Thompson to cover more general boundary conditions and E_s any general function of x. In 1956 Reese and Matlock (16) published a system of curves of non-dimensional parameters for determining deflections and bending moments in piles imbedded in soils with E_s increasing linearly with x, and in 1960 they generalized their technique to handle E_s a function of x and y (17). Davisson and Gill (2) in 1963 used an analog computer to determine moments and deflections in piles embedded in distinctly layered soils, and in 1965 Davisson and Robinson (3) used the same basic technique to determine dimensionless parameters for the determination of deflections and moments in piles partially imbedded in soils having E_s constant and soils having E_s a linear function of x.

The second major area of investigation has been model testing. Wen (24) in 1955 and Kubo (8) in 1965 conducted lateral load tests on sand supported piles instrumented with electrical resistance strain gages.

The third significant area of study has been full scale testing. McCammon and Ascherman (12) in 1953, Matlock and Ripperger (11) in 1956, and McClelland and Focht (13) in 1958 described full scale tests performed on hollow piles instrumented with electrical resistance strain gages. Also Gleser (6) described full scale tests on hollow piles instrumented with trolley mounted dial indicators, and Mason and Bishop (10) and Mason (9) reported the results of full scale tests of hollow piles equipped with an optical deflection indicator and special soil pressure sensors.

The references cited above are representative of the work that has been done on the laterally loaded pile problem. Generally the numerical value or values of the soil modulus of pile reaction, E_s, has been either taken for granted or manipulated with little regard to soil properties to give correlation between calculated and experimental results. The significant exception to this rule is the work done by McClelland and Focht (13). Using pile deflection and reaction values determined from strain gage data and soil properties determined from lab tests, they were able to establish a correlation between E_s and soil properties as determined from consolidated undrained triaxial compression tests. Although their data strongly supported the correlation coefficient, the authors were reluctant to make general conclusions about the nature of the relationship between E_s and soil stress vs strain properties. They also emphasized the significance of further study of this important relationship.

It has been suggested that the photoelastic method might be a valuable tool in the study of laterally loaded piles. The object of this thesis is to demonstrate the utility of the photoelastic method as applied to the laterally loaded pile problem, and to that end the tests described by McClelland and Focht (13) were simulated by a 1/200 th scale photoelastic model. Two important results were obtained from the model testing. First, a comparison of model test results with the full scale demonstrated reasonable agreement. Second, a quantitative evaluation of the model design procedures and test procedures demonstrated that one can reasonably expect successful simulations in subsequent testing.

The model test was conducted in the University of Houston photoelasticity laboratory during the fall semester of 1968. The following sections contain a description of the full scale test results, the model test results, the test procedure and the design and construction of the model pile and model soil.

CHAPTER II

TEST DESCRIPTION

The model test was very much dependent on the full scale test results described by McClelland and Focht (13). The full scale test data consisted of points on a bending moment curve derived from strain gage readings, and stress vs strain properties of the soils at different depths along the pile. The soil properties were determined by testing samples in consolidated undrained triaxial compression tests. Figure 1 shows the pertinent data taken from the paper by McClelland and Focht (13) and Figure 2 gives the pile dimensions.

The full scale pile test was conducted by the Texas A&M Research Foundation in 1952. The test site was in the Gulf of Mexico near New Orleans. The water depth was approximately 30 feet and the pile was driven 75 feet into a normally consolidated clay deposit. A hydraulic jack located 6 feet above the mudline was used to load the pile. The reaction at the top of the pile and the jack load were reacted by a nearby oilwell drilling structure. A complete description of the full scale pile test is given in the Texas A&M Research Foundation Report (22). The soil test data was taken by McClelland and Focht. A continuous Shelby tube boring was made at the site, and the samples were tested in the laboratory.

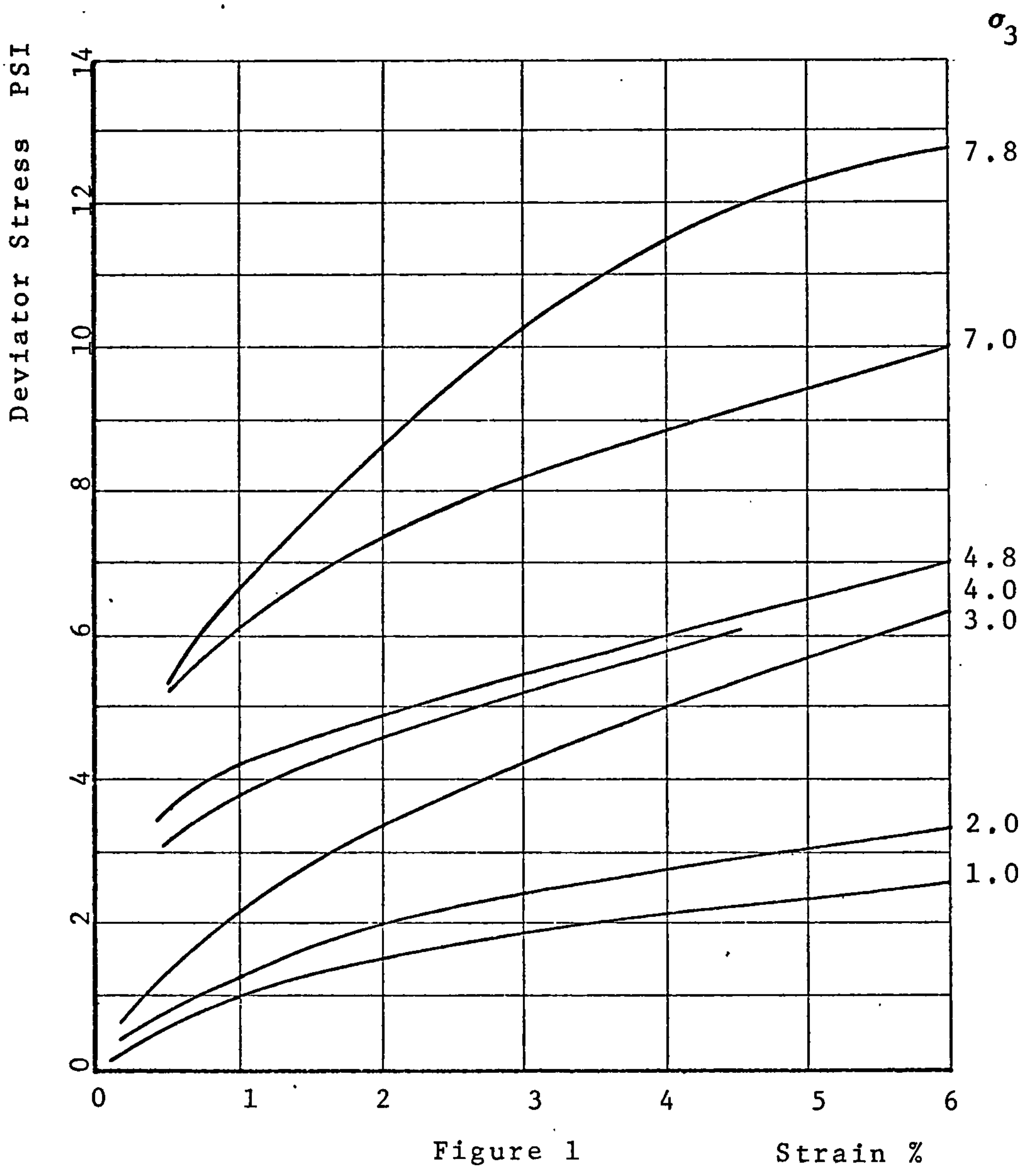

Figure 1

Full Scale Soil Stress vs Strain Properties

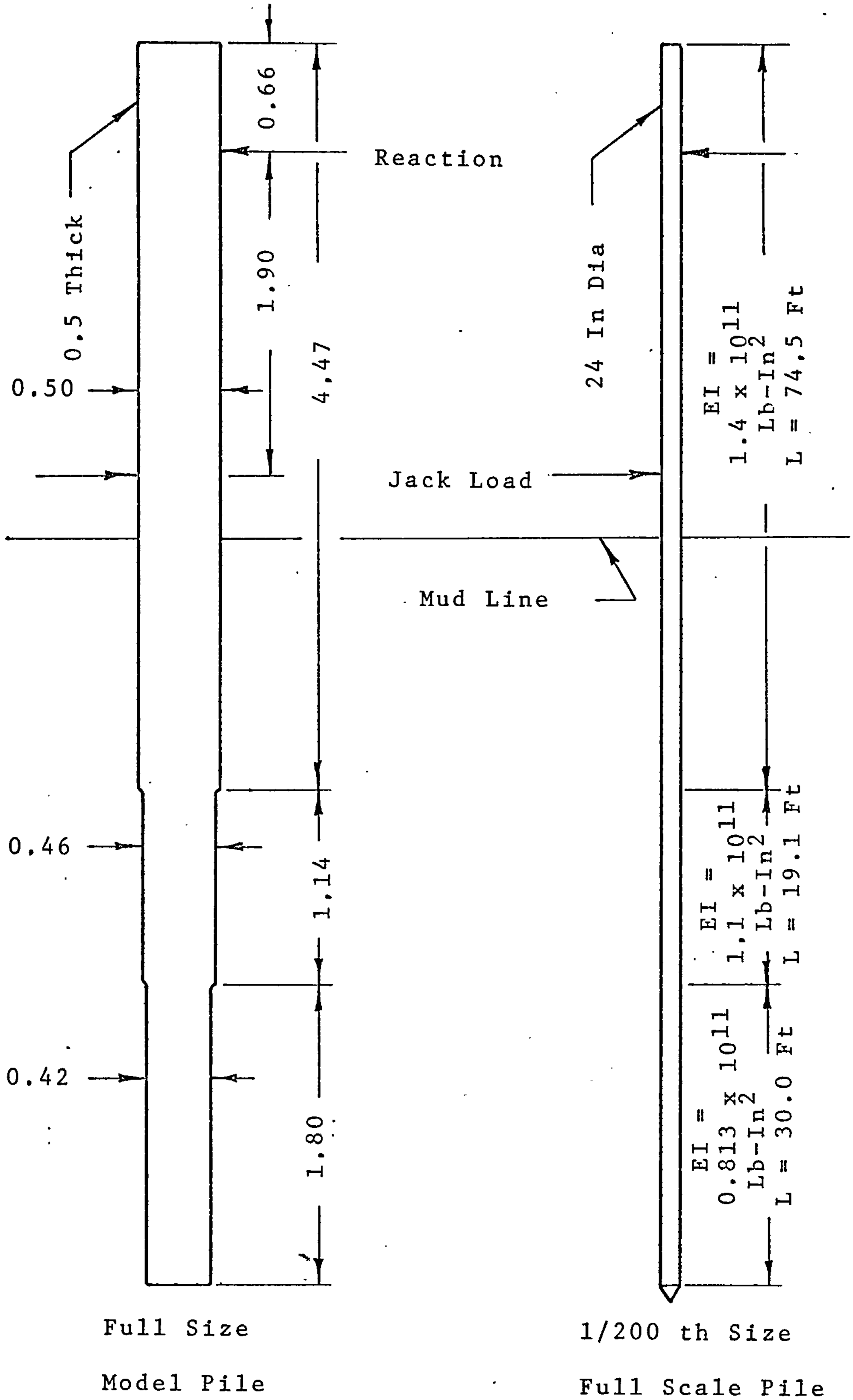

Figure 2

Dimensions and Load Conditions for Test Piles

An exhaustive search of the literature of Civil Engineering revealed no other full scale test results comparable to those described by McClelland and Focht. Soil stress vs strain properties are extremely rare in reports of pile tests.

The model test was conducted using a transmission type polariscope manufactured by Chapman Laboratories of West Chester, Pennsylvania equipped with a loading frame by Scott Aviation Corporation of Boca Raton, Florida. The field of view of the polariscope was 8 inches, therefore, a scale factor of 1/200 was selected giving a model pile approximately 7-1/2 inches long. The details of the model pile are shown in Figure 2 along with the details of the full scale. The model was designed to insure that the two piles would have similar deflection curves. It is relatively easy to demonstrate that such similarity may be attained by satisfying Equation II. Equation II is derived in the Appendix.

$$E_2 I_2 = \frac{E_1 I_1}{K_L{}^2 K_F} \qquad \text{(II)}$$

Where E_2 = Modulus of pile 2
I_2 = Moment of inertia of pile 2
E_1 = Modulus of pile 1
I_1 = Moment of inertia of pile 1
K_L = Length scale factor $\frac{L_1}{L_2}$
K_F = Force scale factor $\frac{P_1}{P_2}$

Equation II is based on the following assumptions:

1. The same length scale factor applies to both x and y

coordinates,

2. Both piles obey the elementary beam equation, Equation III,

$$\frac{d^2y}{dx^2} = \frac{M}{EI} \tag{III}$$

3. The body forces in the pile are negligible.

By evaluating the relative maximum magnitudes of the terms in the differential equation for a beam column with self weight, it can be demonstrated that the body force for the full scale pile of Figure 2 is less than 1% of the applied load [reference Fischer and Ludwig (4)]. For analysis of piles with significant body forces, Equation IV must be satisfied, and the number of independent parameters is reduced by one.

$$\frac{E_1 I_1}{W_1} \; \frac{W_2}{E_2 I_2} = K_L{}^3 \tag{IV}$$

Where W's are weight per unit length.

The modulus of elasticity of the model pile was determined by making tensile and compressive force vs deflection measurements on the test bar shown in Figure 3. From the force vs deflection data of Figure 4, the tensile modulus was determined as 276,000 psi. The compression test was run after completion of all other testing when it was discovered that the compressive modulus was about 15% greater than the tensile modulus. This feature undoubtedly contributed considerably to the overall

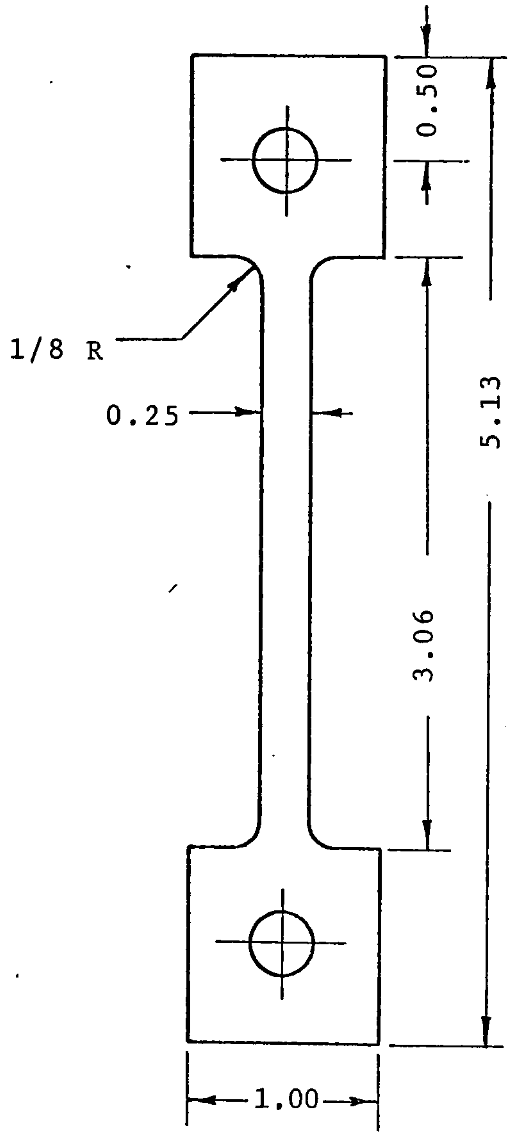

Material 0.37 Thick

Figure 3

Tensile Test Bar

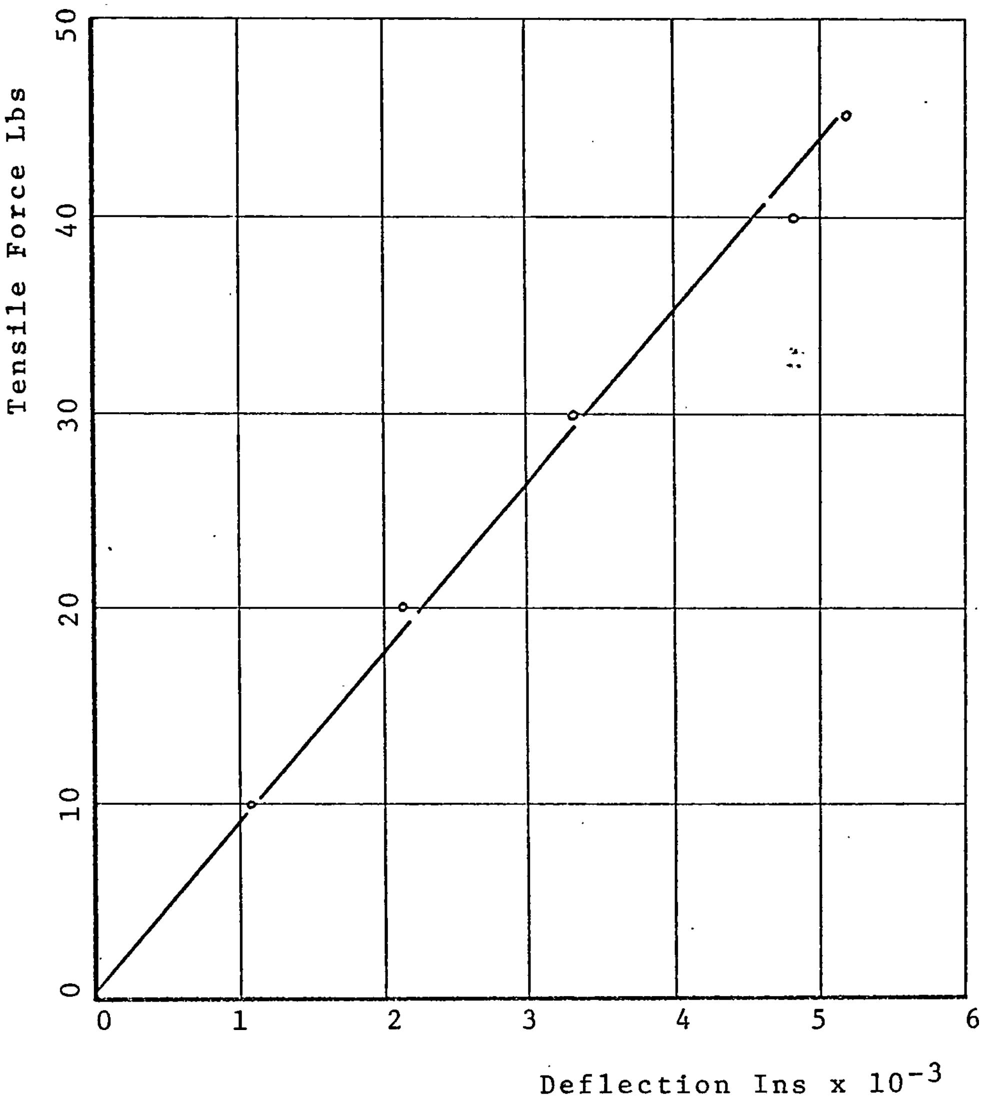

Figure 4

Tensile Test Data

experimental error. The material fringe value was determined with the same test bar. The applied force was increased to a maximum and decreased to zero for two cycles. The force corresponding to each half fringe was recorded. The material fringe value, f, was determined as 65.6 psi-in, and the point data is shown in Figure 5.

The test bar and model pile were cut from portions of the material immediately adjacent to each other. Care was taken to make all opposite surfaces parallel to insure accurate fringe patterns, and edges were made sharp to insure edge definition. The material selected was Shell Epon Resin 815 cured with 5 pph diethylaminopropylamine. The principal considerations in the choice of material were the requirements for high figure of merit,E/f, and availability in thick sections. Representative properties of typical photoelastic materials are given by Dally and Riley (1).

The moment of inertia of the top section of the model pile was chosen more or less arbitrarily. A heavy section gives more fringes but also greater error due to perverted L/D ratio (reference sample calculation V). Having selected a section for the top, K_F was determined to be 2450 using Equation II. The required moments of inertia for sections 2 and 3 were determined using the same thickness and force scale as determined for section 1. Examples of these calculations are given in the Appendix.

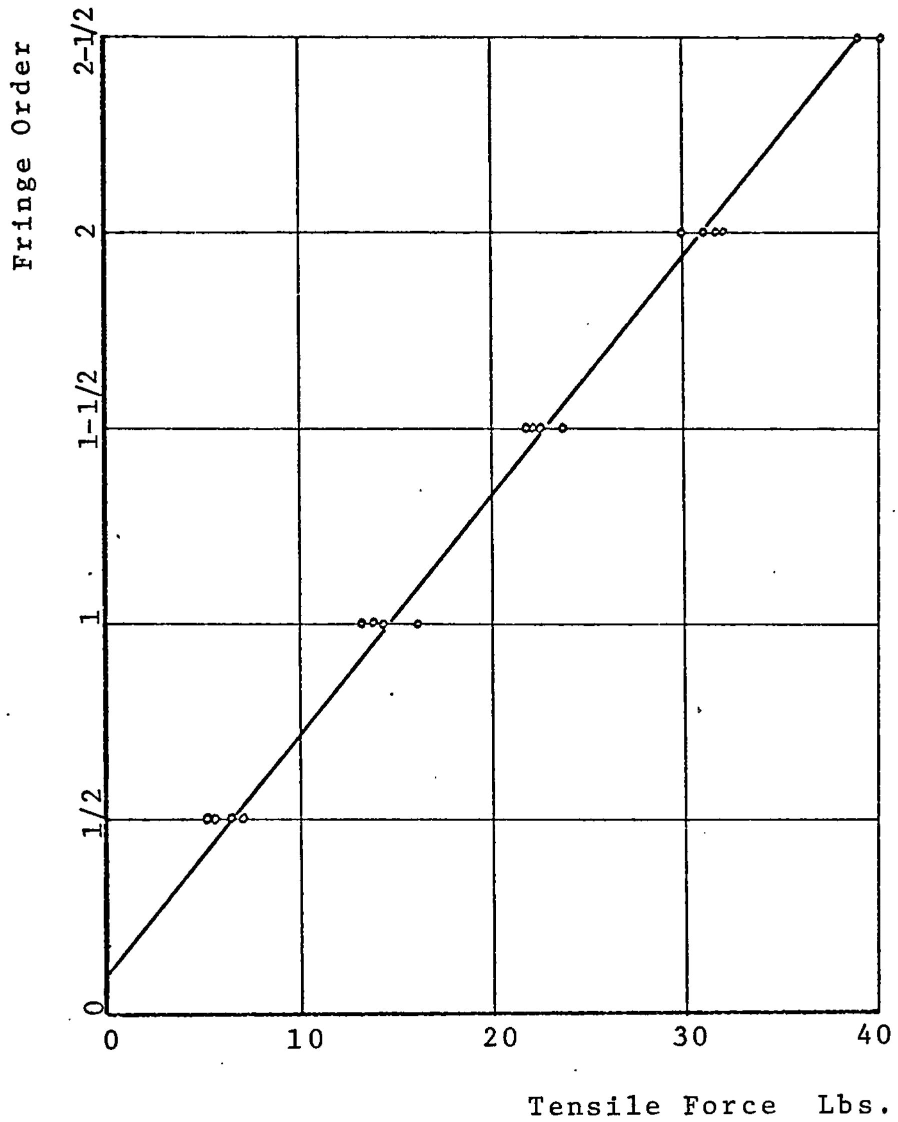

Figure 5

Material Fringe Value Test Data

The scaled applied load was determined as

$$\frac{P_1}{K_F} = \frac{80,000}{2450} = 32.7 \text{ lbs.}$$

In order to apply the scaled load accurately a special leaf spring was designed, built, calibrated, and incorporated into the special loading fixture. An inside micrometer was used to measure the spring deflection and the experimentally determined calibration curve of Figure 6 was used to correlate the micrometer reading with the applied load. Other significant design features of the loading fixture include the vertical adjustment for centering the model in the polarized field, the rotation adjustment for aligning the model parallel to the polariscope axis, and the rigid frame required to support the spring load and soil reactions. These features are all apparent in the photograph of Figure 7 and the schematic of Figure 8. Stiffeners, not shown, were found necessary and added to the fixture.

Possibly the most important consideration of the test was the design of the model soil. It was assumed that if the modulus of the model soil at a given depth corresponded by similitude to the secant modulus of the actual soil as measured in the triaxial test at the corresponding depth, then the model soil would exhibit the proper resistance to pile deflection. The following additional design procedures were established:

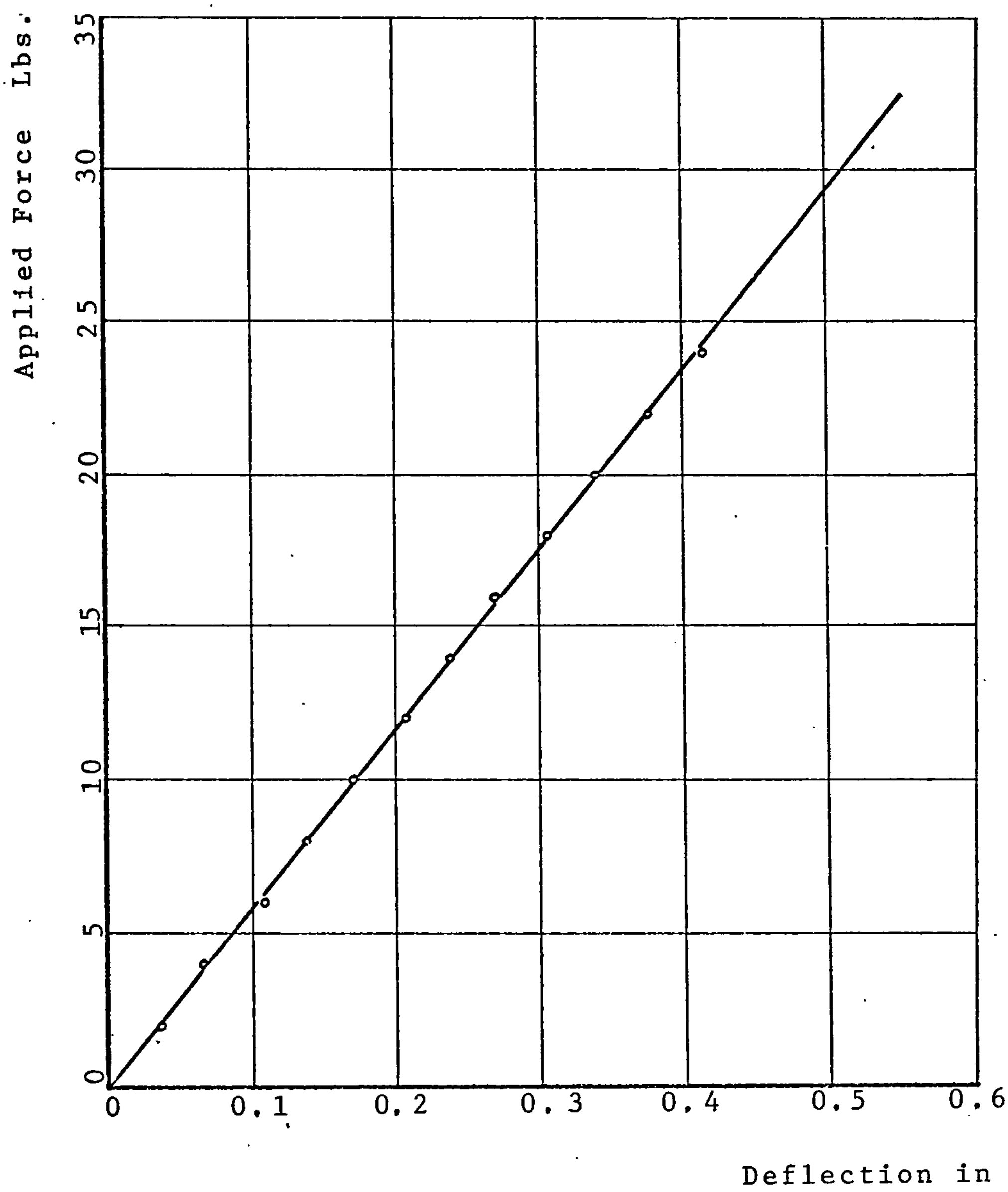

Figure 6

Leaf Spring Calibration Curve

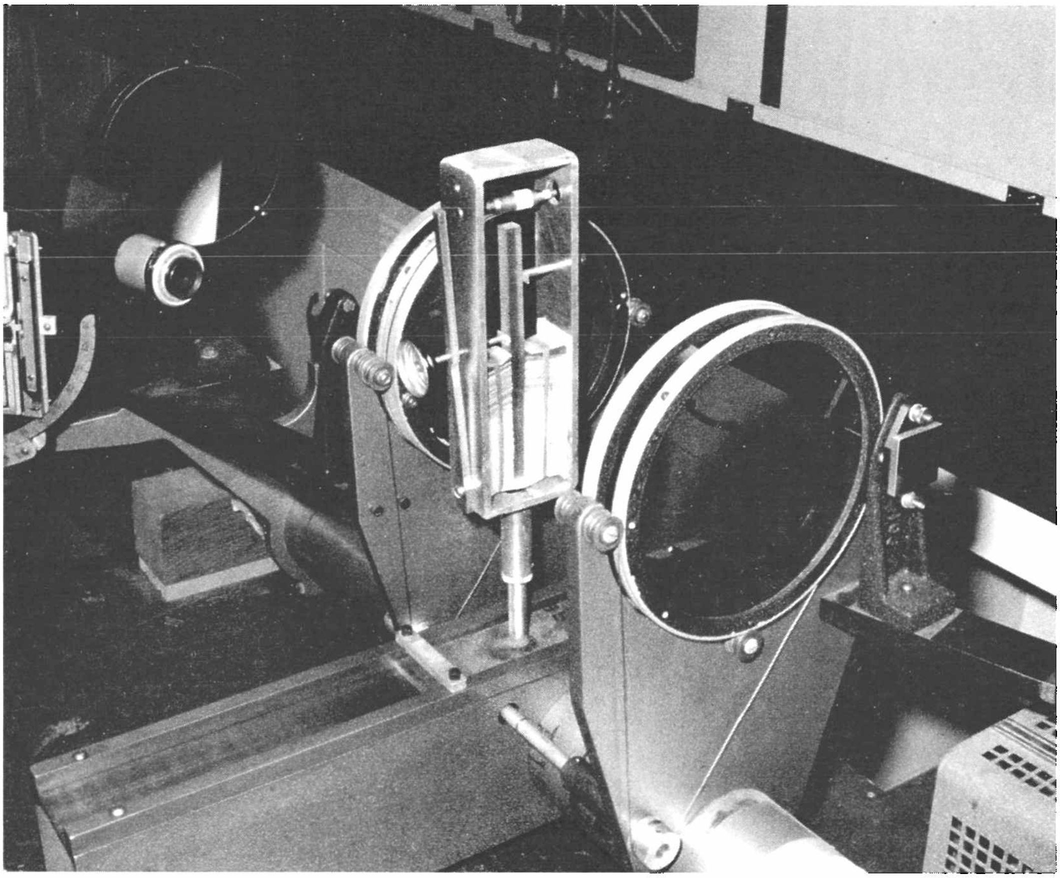

Figure 7

Test Set-up

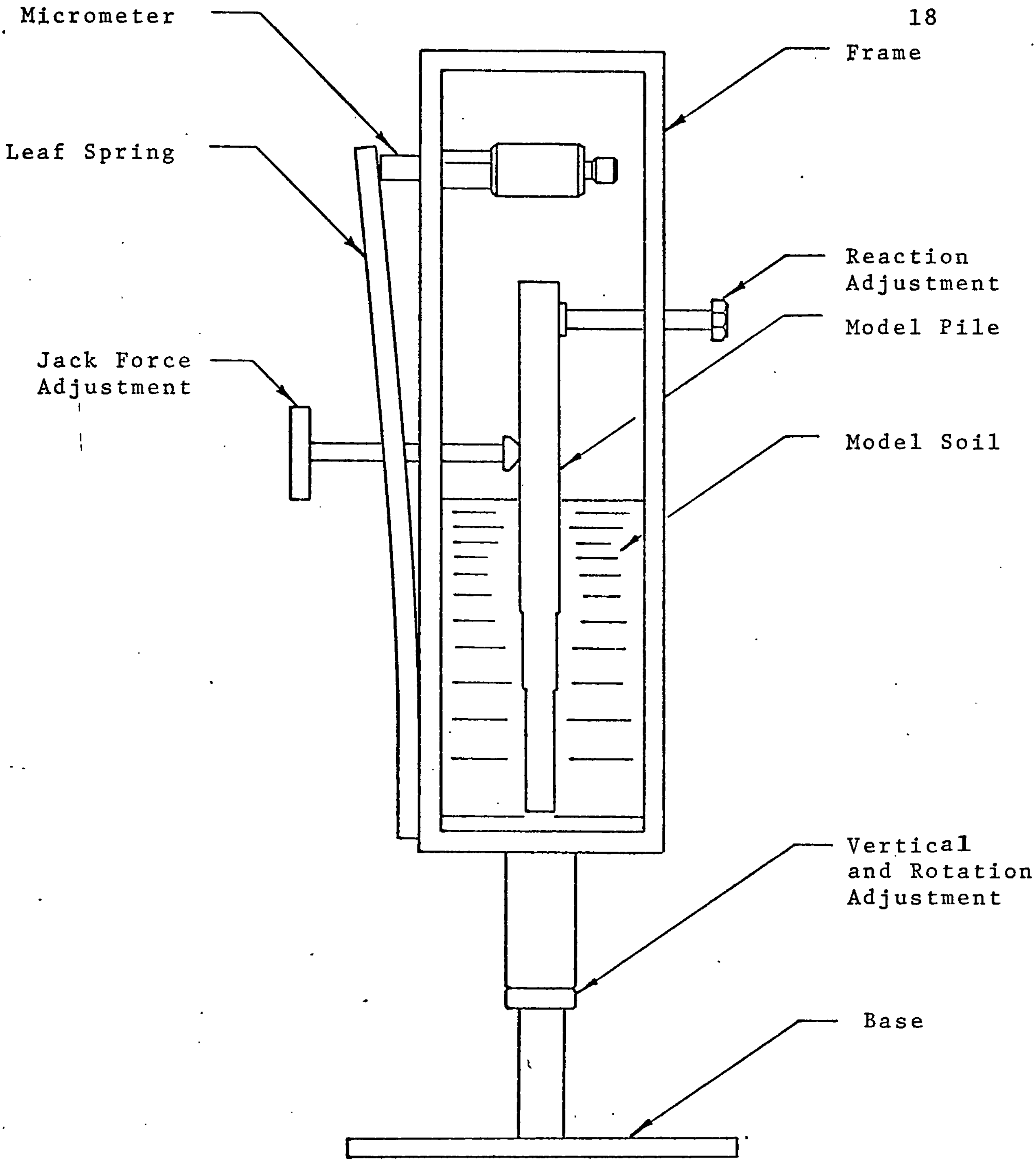

Figure 8

Test Fixture

1. The model soil was constructed of horizontal layers to prevent the development of any flexural strength.

2. The soil modulus gradient was adjusted by leaving voids of proper thickness between layers. An example of the required thickness calculation is given in the Appendix. The full scale soil modulus gradient was determined by fitting a straight line to the modulus vs confining pressure data. The line and data points taken from Reference (13) are given in Figure 9. Figure 10 shows the model soil modulus gradient.

3. The actual soil modulus was selected as the secant modulus at 1% strain. This is consistent with the concept expressed by Terzaghi (21) that the stress affected zone extends only about 3 pile diameters away from the pile.

4. Complete contact between the pile model and soil model (except in void areas) was achieved by fitting all the layers against the pile, clamping the assembly, and then grinding the back side smooth. The pieces were then assembled into the fixture using shims as shown in Figure 11.

5. The modulus of the model soil laminations was determined by taking tensile force vs deflection data for sample strips 1/16 x 1/2 x 2 inches. The three materials chosen were 50 durometer Neoprene, 70 durometer red rubber, and low density polyethylene. The force vs deflection data is shown in Figure 12.

6. The quadrants at 90° to the applied load were left

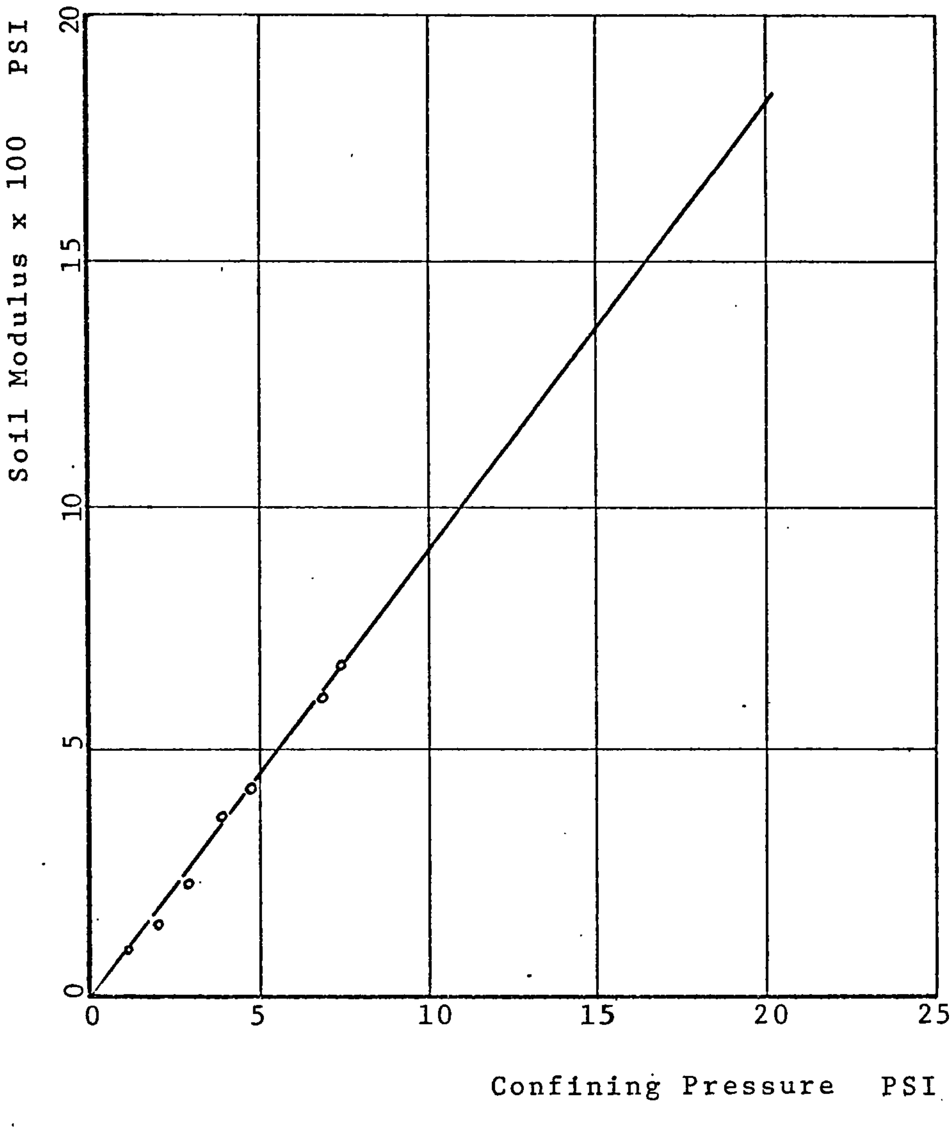

Figure 9

Full Scale Soil Modulus Gradient

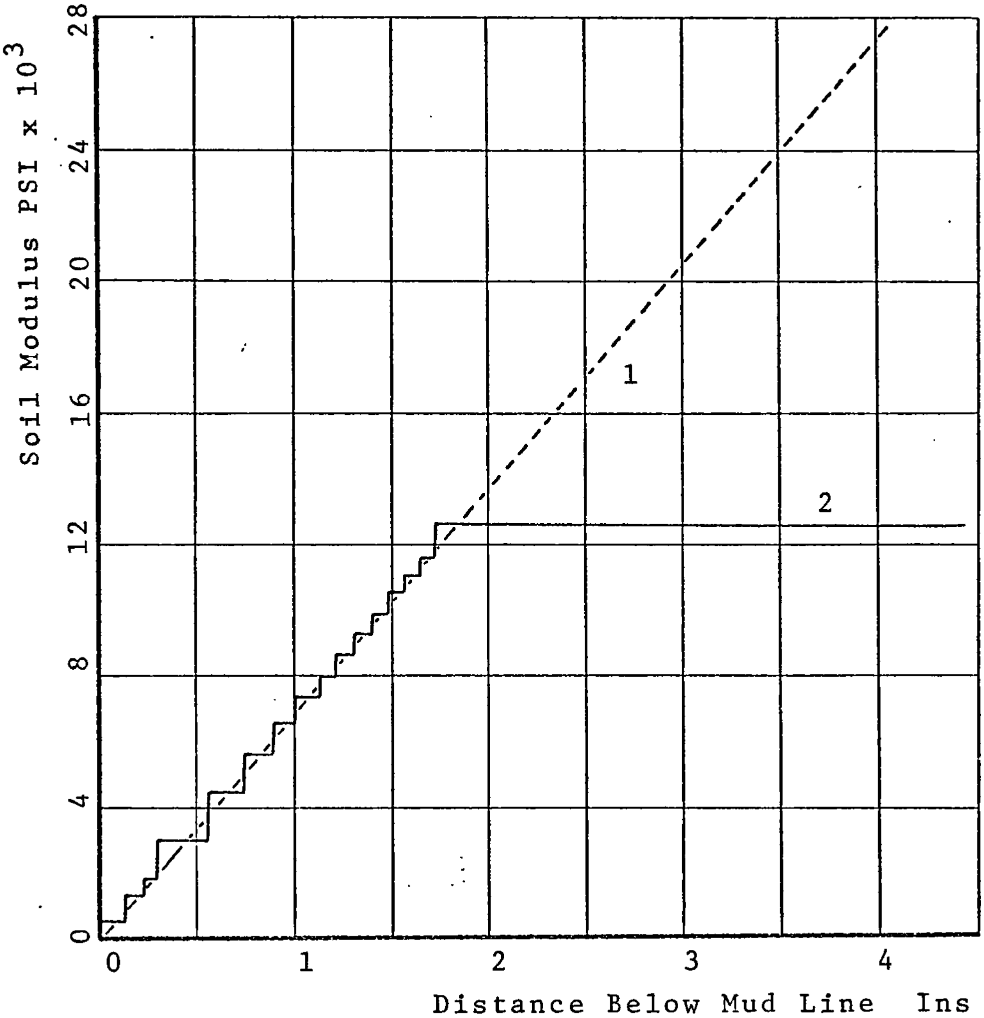

1 Scaled Gradient

2 Actual Model Gradient

Figure 10

Model Soil Modulus Gradient

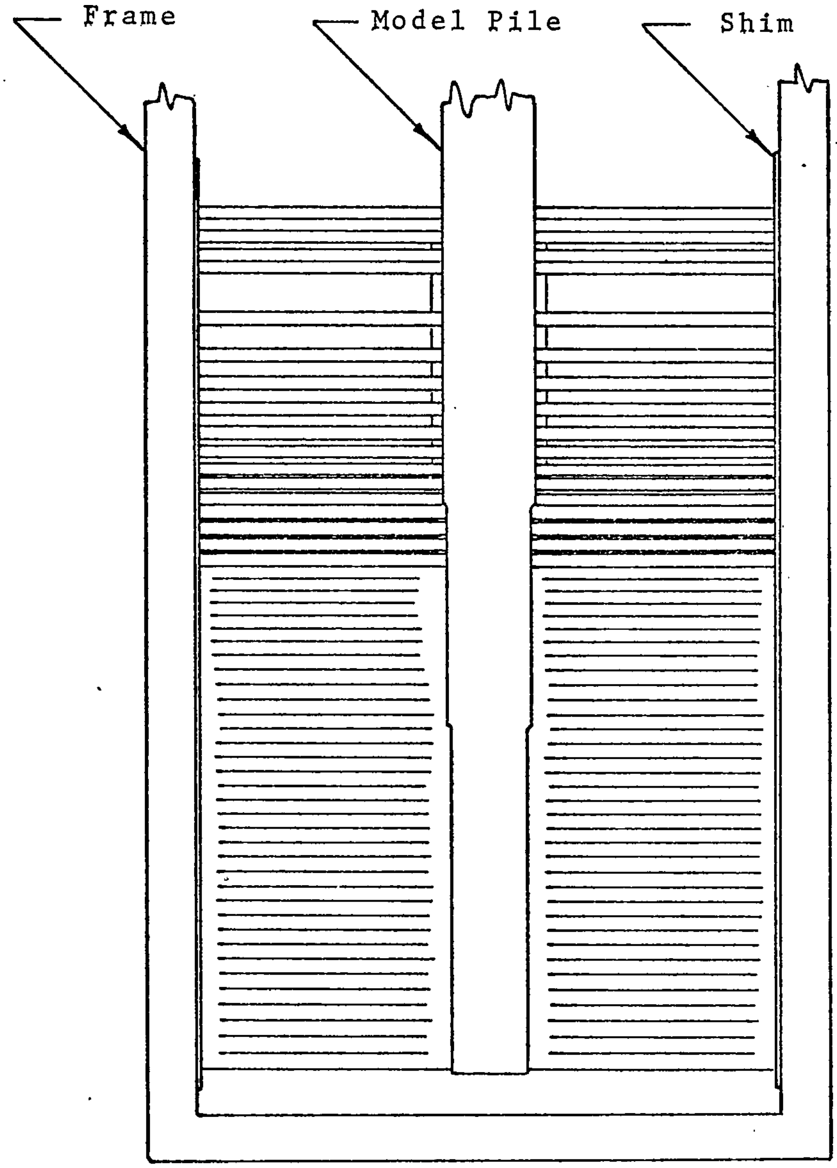

Figure 11

Model Soil Assembly

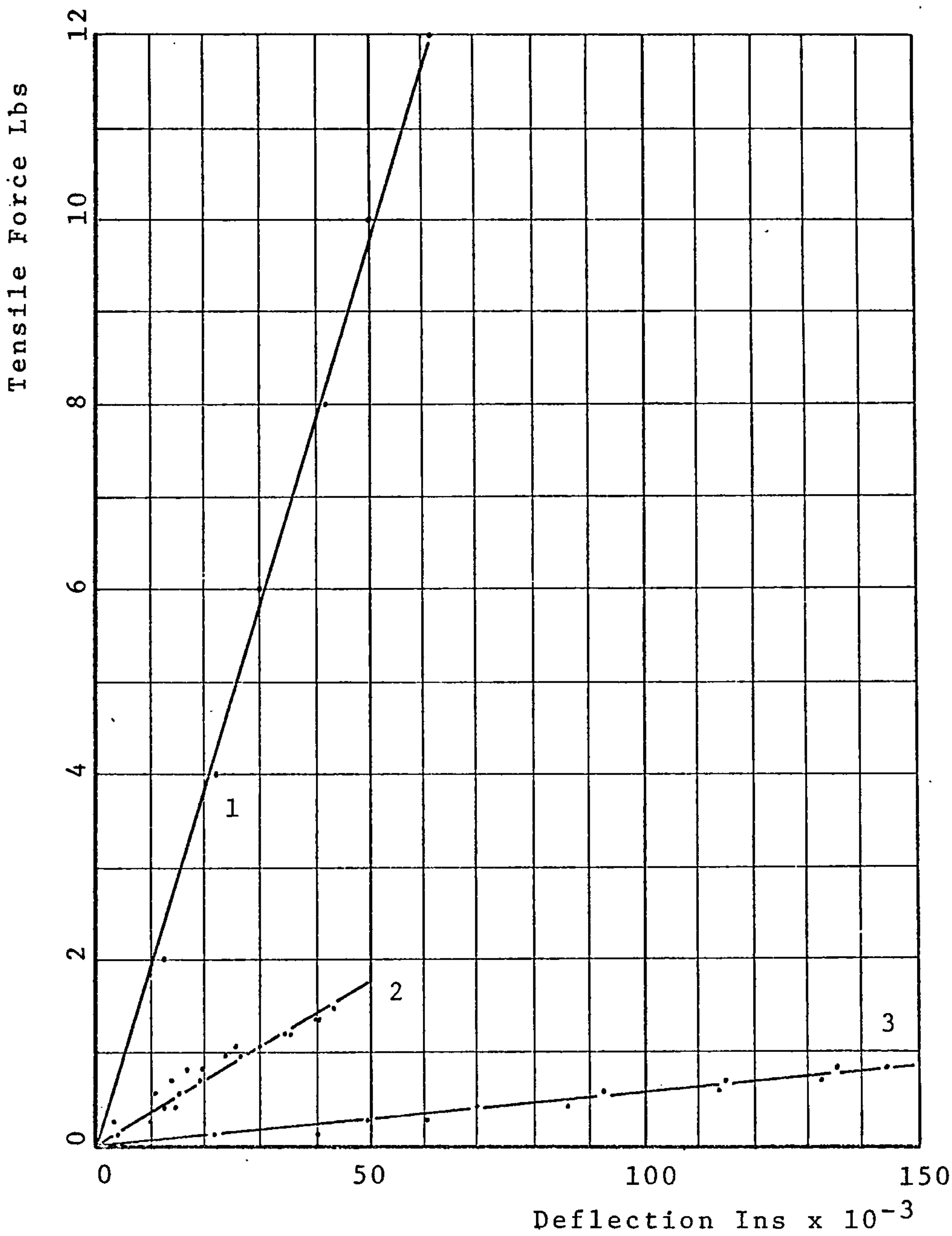

1 Polyethylene
2 Red Rubber
3 Neoprene

Figure 12

Model Soil Materials Properties

void to prevent tensile stresses from being transmitted around the pile and to permit viewing of the photoelastic model.

7. Because of a lack of suitable material it was found impossible to achieve perfect similitude below 1.88 inches in the model soil. Below 1.88 inches the model soil modulus was made constant with depth. This approximation, however, introduces negligible error since the pile exhibits negligible deflection below 1.88 inches. Samples of calculations used to determine the model soil configuration are given in the Appendix.

It is significant that the design procedure outlined above requires no evaluation of the correlation coefficient discussed by McClelland and Focht (13). The significance of the correlation coefficient is illustrated in Figure 13. Figure 13a represents the laboratory compression test and Figure 13b represents the pile test. In each case the soil pressure at the interface is the same. However, it is intuitively apparent that the deflection, δ_o, corresponding to the laboratory test, will be greater than δ_ϵ corresponding to the pile test, even though the two materials have identical mechanical properties. It is the purpose of the correlation coefficient to permit the determination of δ_ϵ from a knowledge of δ_o, and as pointed out by McClelland and Focht, the difference in δ_o and δ_ϵ would seem to arise out of the difference in the stress conditions and the masses of materials involved.

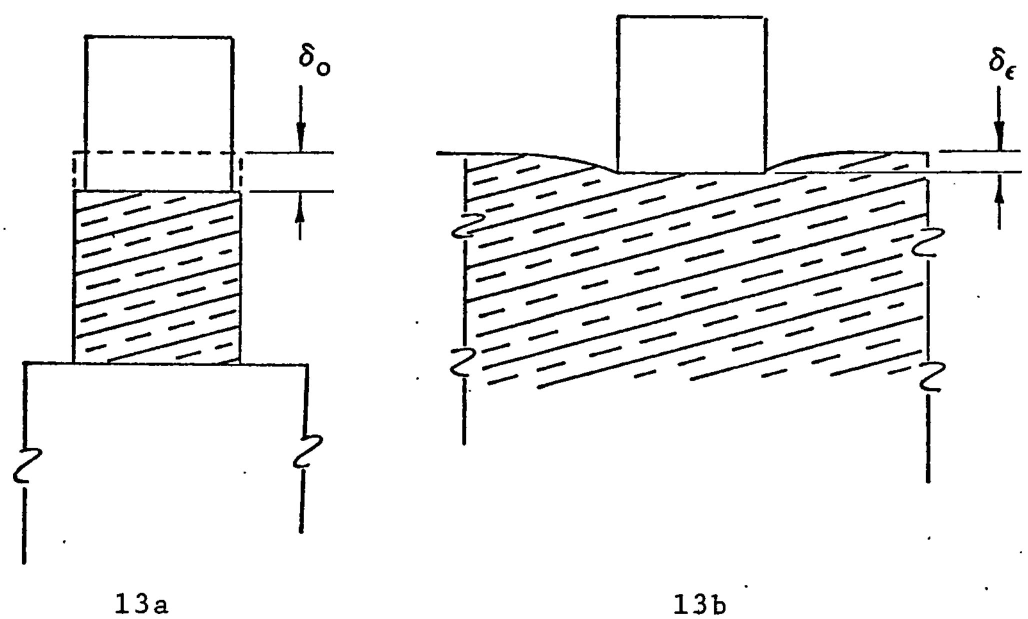

Figure 13

Soil Modulus of Pile Reaction

Correlation Coefficient Analog

The 7 design considerations listed above permit the simulation of the full scale test without regard to the correlation coefficient. The conditions of the pile test were simulated by the model test, and the conditions of the laboratory soil tests were simulated by the force vs deflection tests on the model soil materials. (The assumption that the soil model materials show approximately the same modulus in tension and compression for very low strains is supported by The Handbook of Molded and Extruded Rubber (7) provided the shape factor is near zero). Thus for this type of experiment the correlation coefficient is a dependent variable and can be evaluated in terms of the other test parameters and test results just as was done with the full scale test.

The actual evaluation of the photoelastic fringe patterns was accomplished using circularly polarized monochromatic light from a mercury vapor lamp with a green filter. For the zero load condition white light was used to help evaluate the partial fringe orders present due to initial and residual stresses. Using the test bar of Figure 3, an approximate color scale was obtained which was used to determine values of fringe order less than one. A thorough discussion of fringe determination by color matching is given by Frocht (5).

With the model in the loaded condition, fringe orders were determined using the monochromatic light. Coordinates were measured corresponding to each point where a fringe contacted the edge of the model. All points were measured with respect to the top reaction point.

The Tardy compensation technique was used to determine the fringe value for every 1/4 fringe. Tardy compensation is accomplished by first setting up the polariscope in a standard crossed configuration with the polarizer aligned with the direction of the maximum principal stress at the point of interest. In this configuration the angular coordinate of the analyzer, θ , is designated zero. With θ at zero the fringe order, n , on either side of the point of interest is determined. The analyzer is then rotated through some angle θ, less than 180°, until a fringe migrates to the point of interest. The fringe value at the point, n', is then determined from Equation V.

$$n' = n+\frac{\theta}{\pi} \tag{V}$$

Where n' = Partial fringe order at point of interest
n = Integral fringe order
θ = Tardy angle

As a matter of procedure the analyzer was set to angles corresponding to every 1/4 fringe and corresponding coordinates were measured as dependent variables. A thorough discussion of Tardy compensation is given by Dally and Riley (1).

As a last step the analyzer was returned to the zero position and measurements were repeated to check for optical and mechanical creep and repeatability. No effort was made to determine the isoclinics because only the edges of the model were of interest; and since the shear stress was zero on the model edges, the direction of principal stress was known.

CHAPTER III

TEST RESULTS

Fringe patterns for the zero load and design load are shown in Figure 14a and Figure 14b respectively. The x coordinates of the fringe pattern of Figure 14b are given in Table I. Figure 15 gives plots of fringe order vs x coordinate for the following cases:

15a. Jack side - zero load
15b. Jack side - full load
15c. Reaction side - zero load
15d. Reaction side - full load

As with most experimental work, the results were not exactly as anticipated. It is apparent from Figure 15 and Figure 14b that the fringe pattern is confused on the jack side above the mudline and on the reaction side below the mudline. In the first case the fringes are too close to be resolved, and in the second case the points of contact between the soil and pile create localized stresses. This effect is readily apparent in Figure 14b. The results of the test must therefore be evaluated on the basis of the fringe pattern on the reaction side above the mudline and on the jack side below the mudline. Using the data for these areas and correcting for the initial and residual fringes, the composite n vs x diagram of Figure 16 was obtained. Also plotted on Figure 16 are full scale data points converted to fringe values. To effect this data conversion

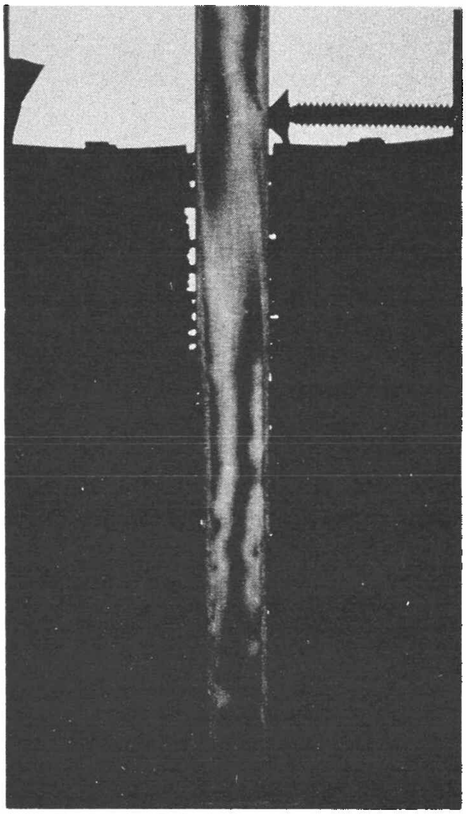

14a Zero Load

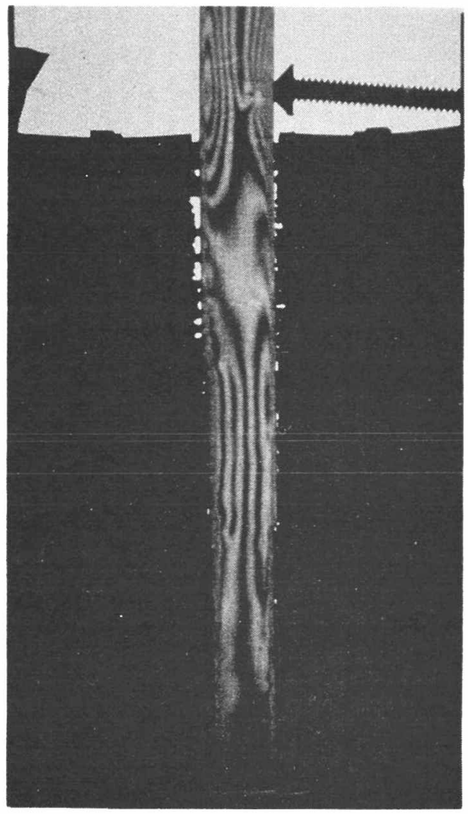

14b Full Load

Figure 14

Model Fringe Patterns

TABLE I

Measured Values of Model Pile Fringe Order

	θ = 0°		θ = 45°		θ = 90°		θ = 135°		θ = 0°	
	x	n	x	n	x	n	x	n	x	n
	1/8	- 1	1/4	- 1 1/4	5/16	- 1 1/2	3/8	- 1 3/4	1/8	- 1
	1/2	- 2	9/16	- 2 1/4	5/8	- 2 1/2	11/16	- 2 3/4	7/16	- 2
	3/4	- 3	7/8	- 3 1/4	1	- 3 1/2			3/4	- 3
	2 1/4	- 1	2 3/8	+ 1/4	2 3/8	+ 1/2	2 5/8	+ 3/4		
	2 3/8	0	2 1/2	+ 1 1/4	2 1/2	+ 1 1/2	2 3/4	+ 1 3/4		
JACK	2 1/2	+ 1	2 11/16	+ 2 1/4	2 11/16	+ 2 1/2				
	2 3/4	+ 2	2 7/8	+ 3 1/4	2 13/16	+ 3 1/2			2 3/4	+ 2
SIDE	2 7/8	+ 3	3 5/16	+ 3 1/4	3 3/16	+ 3 1/2				
	3 5/16	+ 3	3 5/8	+ 2 1/4	3 9/16	+ 2 1/2	3 3/4	+ 1 3/4		
	3 5/8	+ 2			4	+ 1 1/2	4 3/16	+ 1 3/4		
	5	+ 2	4 7/8	+ 2 1/4	4 3/4	+ 2 1/2				
	5 7/16	+ 1	5 1/4	+ 1 1/4	5 3/16	+ 1 1/2	5 1/8	+ 3/4		
	3/8	+ 1	5/16	+ 3/4	9/16	+ 1 1/2	7/16	+ 1 1/4		
	3/4	+ 2	5/8	+ 1 3/4	13/16	+ 2 1/2	3/4	+ 2 1/4		
	1 1/8	+ 3	1	+ 2 3/4	1 5/16	+ 3 1/2	1 3/16	+ 3 1/4		
	1 7/16	+ 4	1 5/16	+ 3 3/4	1 9/16	+ 4 1/2	1 1/2	+ 4 1/4		
	1 11/16	+ 5	1 11/16	+ 4 3/4	2 1/16	+ 4 1/2	2 1/16	+ 4 1/4		
	1 7/8	+ 5	1 15/16	+ 4 3/4	2 3/16	+ 3 1/2	2 1/4	+ 3 1/4		
REACTION	2 1/8	+ 4	2 1/8	+ 3 3/4	2 3/8	+ 2 1/2	2 1/2	+ 2 1/4		
	2 5/16	+ 3	2 5/16	+ 2 3/4	2 9/16	+ 1 1/2	2 9/16	+ 1 1/4		
SIDE	2 1/2	+ 2	2 1/2	+ 1 3/4	2 11/16	+ 1/2	2 3/4	+ 1/4		
	5 1/2	0	6	- 1/4	5 1/2	- 1/2	5 5/8	- 3/4		

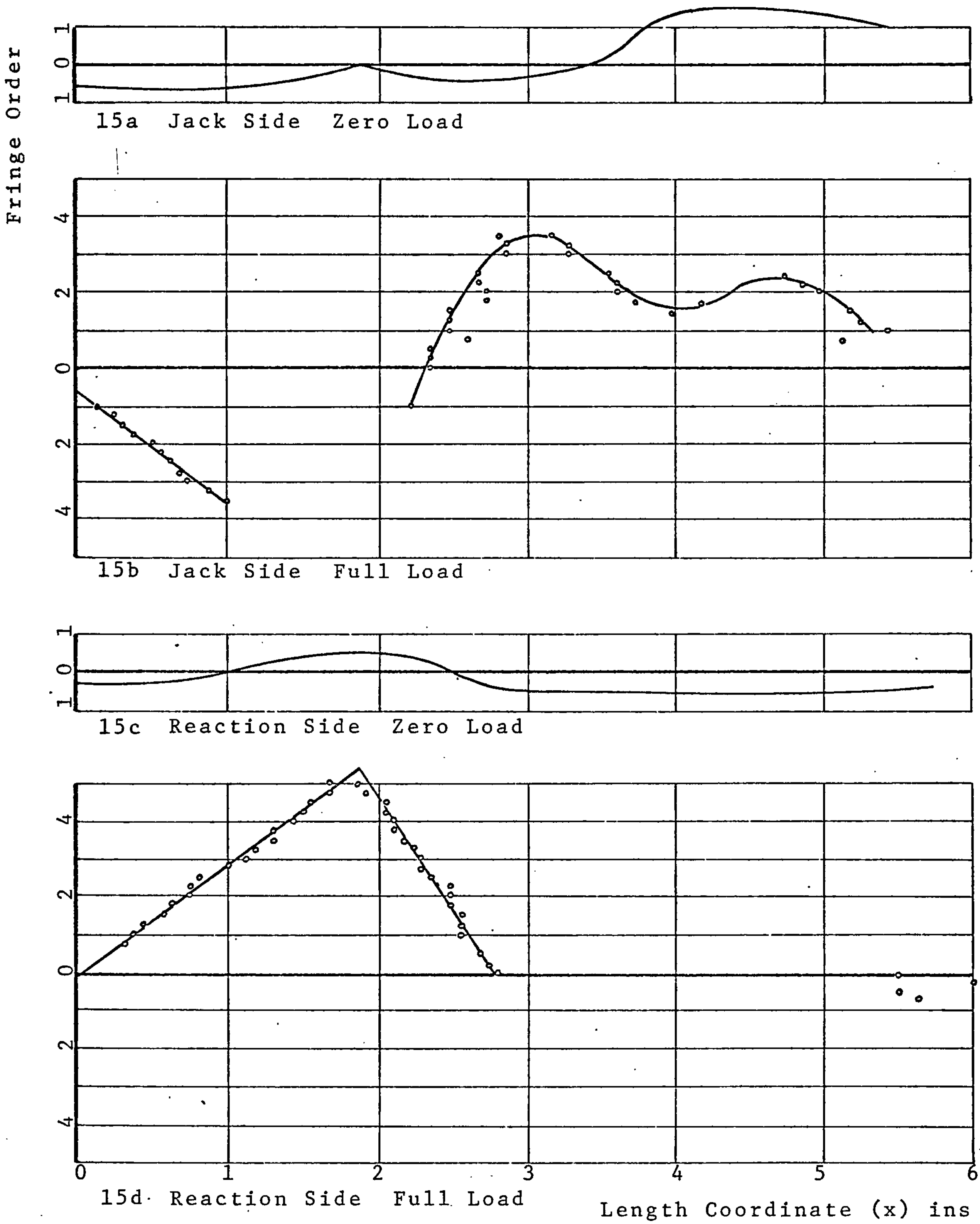

Figure 15

Fringe Data

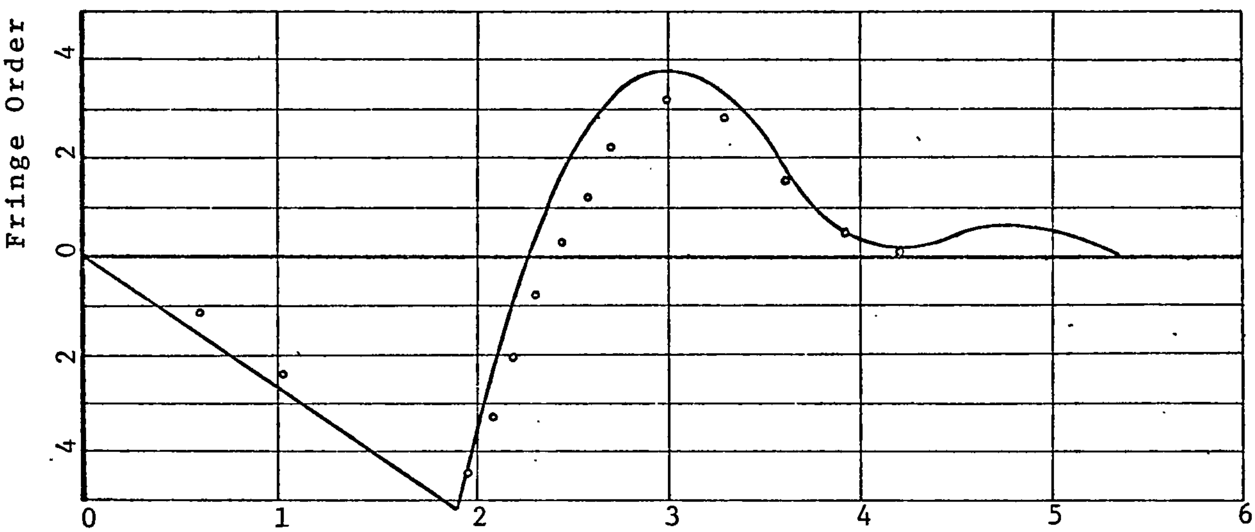

Length Coordinate (x) ins

• Full Scale Data Points

Figure 16

Corrected Composite Fringe Data

Equation VI was used.

$$n = \frac{htM_1}{2fI_2K_FK_L} \qquad \text{(VI)}$$

Where M_1 = Full scale moment
f = Model fringe value
n = Fringe order
I_2 = Model pile moment of inertia
h = Model pile height
t = Model pile thickness
K_L = Length scale factor
K_F = Force scale factor

Equation VI is applicable to areas of the pile where the minimum principal stress, q, is zero (namely the reaction side above the mudline and the jack side below the mudline). For these areas the fringe value is given by Equation VII.

$$n = \frac{\sigma t}{f} \qquad \text{(VII)}$$

Where σ = Bending stress in the model pile,

and the model pile bending stress is given by Equation VIII.

$$\sigma = \frac{M_1 h}{2I_2K_FK_L} \qquad \text{(VIII)}$$

Equations VII and VIII can be solved for n in terms of M_1 thus giving Equation VI and permitting a direct comparison of model test results with full scale test results. As can be seen from Figure 16 the model data and full scale data correspond within about 15%.

Figure 17 compares the model and full scale deflection curves. Both were derived from their respective moment curves. The full scale deflections were scaled directly from Reference (13), and the model deflections were obtained by double graphical integration of Figure 16. A polar planimeter accurate to the nearest 1/1000 of a square inch was used to perform the integration.

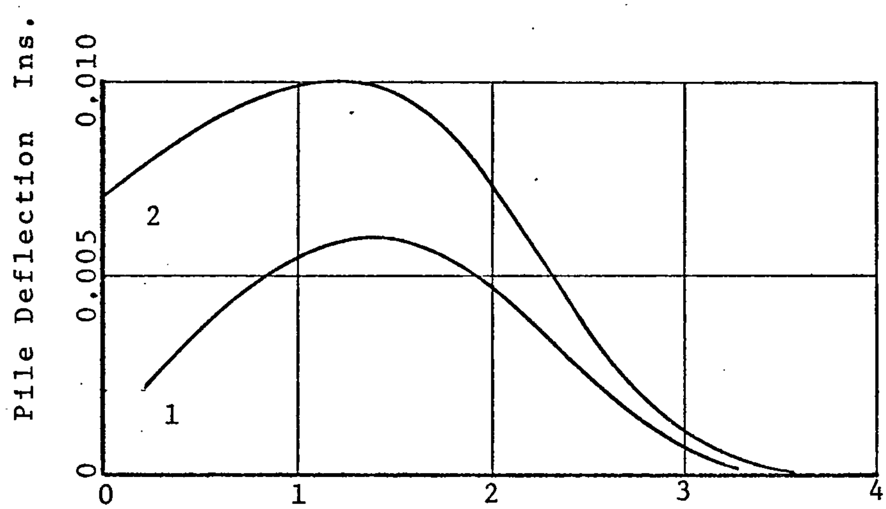

Length Coordinate (x) ins.

1 Full Scale Deflection (Scaled)

2 Model Deflection

Figure 17

Pile Deflection Curves

CHAPTER IV

CONCLUSIONS

Based on the results presented in Figure 16 the following conclusions are justified:

1. For at least one case it is possible to achieve reasonable agreement between full scale tests and photo-elastic model tests of a laterally loaded pile.

2. A laterally loaded pile test can be simulated by a model without resorting to a correlation coefficient as developed by McCelland and Focht.

3. Further testing of photoelastic piles and refinement of test procedure are warranted.

Each of the many facets of this experiment could be refined to improve the overall accuracy of the simulation. The most obvious improvement would be the model soil. By use of more materials and thinner laminations the reaction below the mudline could be smoothly distributed as in the full scale case. Under such conditions it should be possible to obtain smooth curves of p-q (principal stress difference) for both the jack side and the reaction side. Algebraic addition of the two curves would yield a curve of soil reaction which could be integrated over the length as a check for equilibrium of forces and moments.

The data gathering technique might be considerably improved. Much better fringe data might be obtained by photographing a model of improved clarity at 10 different analyzer positions. The photographs could be enlarged and superimposed using an optical comparator. Thus fringes could easily be determined to the nearest 0.1 fringe and coordinates to the nearest 0.010 inches instead of the 1/4 fringe and 1/32 inch as was achieved. This method was attempted, however, due to the poor clarity of the model it was impossible to obtain satisfactory photographs at analyzer angles other than zero (dark background).

Model test results might be improved by correcting for the effects of shear strain. For example for this test the shear strain was of the order of 10 times more significant in the model than in the full scale pile due to the perverted L/D ratio. This effect is illustrated in the sample calculation Section V.

The model pile material was tested in compression and found to exhibit a modulus about 15% higher than the tensile modulus. It should be noted that compression testing is subject to greater error than tensile testing. Any difference in tensile and compressive modulus could be expected to cause considerable error in scaling calculations as well as model pile behavior. Probably with judicious selection of material and improved compression test procedures the problem could be considerably reduced.

The influence of the dual modulus effect on pile behavior can be evaluated by the method of transformed sections as discussed by Timoshenko (23). By this technique the section of the pile is converted to an equivalent section with uniform modulus. In order to use the technique, the neutral axis must be located. Since the sign of the bending stress differentiates the two moduli, the neutral axis is the demarcation between them. By integrating the bending stress over the cross section and equating the result to zero the neutral axis can be located. For this purpose it is reasonable to assume a linear variation of strain over the section as illustrated in Figure 18a. This assumption is justified for small strains and gives the stress distribution of Figure 18b. It is relatively easy to demonstrate that the distance to the neutral axis, a, is given by Equation IX.

$$a = h\left(\phi - \sqrt{\phi^2 - \phi}\right) \tag{IX}$$

Where $\phi = E_2/(E_2 - E_1)$
E_2 = the greater modulus
E_1 = the lesser modulus
h = the pile height

For the model pile the lesser modulus was approximately 85% of the greater and applying Equation IX $a/h = 0.53$. Using this value the transformed section technique yields an effective stiffness, EI, of 1575 lb-in^2, or about 12% greater than the uncorrected value. By adjusting Figure 16 to reflect this correction, the agreement could be significantly improved.

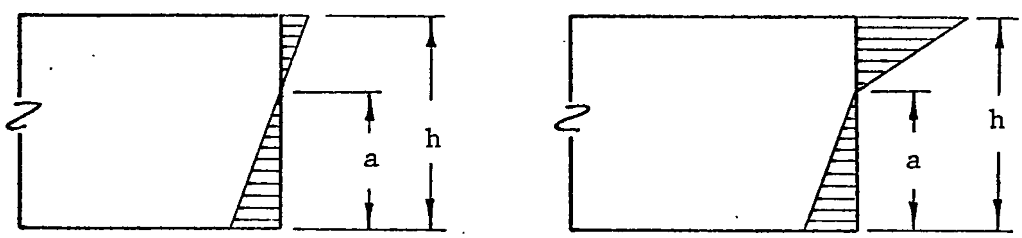

18a Strain Distribution   18b Stress Distribution

Figure 18

Stress and Strain Distribution for Beam

With Dual Modulus Effect

It is apparent from Figure 17 that the model deflection curve is about 67% in error at the point of maximum deflection. This magnitude of error is considered reasonable in view of the following:

1. Considerable error can accrue from graphical integration of a curve that has distortion and magnitude errors.

2. The model deflection curve was subject to error due to shear strain.

3. The model applied load was subject to error due to the dual modulus effect.

4. The model moment curve was subject to error due to inaccurate fringe order readings.

Since it has been shown that all of the above experimental errors are subject to considerable improvement by refinement of procedure, it is reasonable to assume that deflection curves much more accurate than Figure 17 might be easily obtained.

Of course all of the measured values were subject to experimental error, however, as apparent in Figures 4, 5, 6, and 12, the scatter was reasonably low. Most measured values showed standard deviations less than 5% of the measured value. [reference Schenck (20)].

Finally some error was inherent in the full scale data. Measured values of shear and values obtained by differentiation of the full scale moment curve showed as much as 12% discrepancy.

In conclusion it should be pointed out that the objective of the testing was achieved in that the full scale test results for a laterally loaded pile were simulated with reasonable accuracy. It should also be pointed out that although the scope of the test is very limited, additional testing is warranted to further refine and evaluate the photoelastic method of pile analysis.

B I B L I O G R A P H Y

BIBLIOGRAPHY

1. Dally, James W., William F. Riley. Experimental Stress Analysis, St. Louis: McGraw-Hill Book Company, 1965.

2. Davisson, M. T., H. L. Gill. "Laterally Loaded Piles in a Layered Soil System," Proceedings of the American Society of Civil Engineers, Vol. 89 No. SM3 (1963), pp. 63-94.

3. Davisson, M. T., K. E. Robinson. "Bending and Buckling of Partially Embedded Piles," Proceedings of the Sixth International Conference on Soil Mechanics and Foundation Engineering, Vol. 2, Division 3-6 (1965), pp. 243-246.

4. Fischer, William, Milton Ludwig. "Design of Floating Vessel Drilling Riser," Proceedings of Society of Petroleum Engineers of AIME, (October, 1965).

5. Frocht, Max Mark. Photoelasticity, Vol. I, New York: John Wiley and Sons, Inc., 1941.

6. Gleser, Sol M. "Lateral Load Tests on Vertical Fixed-Head and Free-Head Piles," ASTM Special Publication, No. 154 (1953), pp. 75-101.

7. Goodyear Tire and Rubber Company, Inc. Handbook of Molded and Extruded Rubber, First Edition (1949).

8. Kubo, K. "Experimental Study of the Behavior of Laterally Loaded Pile," Proceedings of the Sixth International Conference on Soil Mechanics and Foundation Engineering, Vol. 2, Division 3-6 (1965), pp. 275-279.

9. Mason, Harold G. "Field Test on Laterally Loaded Piles in Sand and Clay," ASTM Special Publication, No. 206 (1957).

10. Mason, H. G., J. A. Bishop. "Measurement of Earth Pressure and Deflections Along the Embedded Portion of a 40 Foot Steel Pile," ASTM Special Publication, No. 154A (1953), pp. 1-21.

11. Matlock, Hudson, E. A. Ripperger. "Procedures and Instrumentation for Tests on a Laterally Loaded Pile," Proceedings of the Eighth Texas Conference on Soil Mechanics and Foundation Engineering, (1956), pp. 1-39.

12. McCammon, G. A., J. C. Ascherman. "Resistance of Long Hollow Piles to Applied Lateral Loads," ASTM Special Publication, No. 154 (1953), pp. 3-9.

13. McClelland, Bramlette, John A. Focht, Jr. "Soil Modulus for Laterally Loaded Piles," Transactions of the American Society of Civil Engineers, Vol. 123 (1958), pp. 1049-1063.

14. Palmer, L. A., P. P. Brown. "Analysis of Pressure Deflection, Moment and Shear by the Method of Difference Equation," ASTM Special Publication, No. 154A (1953), pp. 22-32.

15. Palmer, L. A., J. B. Thompson. "The Earth Pressure and Deflection Along the Embedded Length of Piles Subjected to Lateral Thrust," Proceedings, Second International Conference on Soil Mechanics and Foundation Engineering, Vol. V (1948), pp. 156-161.

16. Reese, Lyman C., Hudson Matlock. "Non-Dimensional Solutions of Laterally Loaded Piles with Soil Modulus Assumed Proportional to Depth," Proceedings of Eighth Texas Conference on Soil Mechanics and Foundation Engineering, (1956), pp. 1-41.

17. Reese, Lyman C., Hudson Matlock. "Numerical Analysis of Laterally Loaded Piles," Proceedings Second Structural Division Conference on Electronic Computation, (1960), pp. 667-668.

18. Rifadt, Ing. J. Die Spundwand als Erddruckproblem, A. F. Gebr. Leeman and Company, Zurich, Switzerland (1935).

19. Ripperger, E. A. "Discussion of American Society of Civil Engineers, Paper No. 2954," Transactions of the American Society of Civil Engineers, Vol. 123 (1958), P. 1074.

20. Schenck, Hilbert, Jr. Theories of Engineering Experimentation, New York: McGraw-Hill Book Company, 1961.

21. Terzaghi, Karl. "Evaluation of Coefficients of Subgrade Reaction," Geotechnique Institution of Civil Engineers, Vol. V (1955), pp. 297-326.

22. Texas A and M Research Foundation. An Investigation of Lateral Loads on a Test Pile, Project 31 (1952).

23. Timoshenko, S. Strength of Materials Part II, New York: D. Van Nostrand Company, 1930.

24. Wen, R. K. L. "Model Studies of Laterally Loaded Pile Foundation," Proceedings of Thirty-Fourth Annual Meeting of Highway Research Board, Vol. 34 (1955), pp. 140-152.

APPENDIX

SAMPLE CALCULATIONS

I. Similarity Requirements

Consider two rectangular coordinate systems (x_1, y_1) and (x_2, y_2) such that by definition $K_L = x_1/x_2 = y_1/y_2$. Then from the calculus, the following coordinate relationships may be obtained:

$$\frac{dy_1}{dx_1} = \frac{dy_1}{dx_2}\frac{dx_2}{dx_1} = \frac{1}{K_L}\frac{dy_1}{dx_2} = \frac{1}{K_L}\frac{d}{dx_2}(K_L y_2)$$

$$\frac{dy_1}{dx_1} = \frac{1}{K_L}\left(K_L \frac{dy_2}{dx_2}\right) = \frac{dy_2}{dx_2}$$

Repeating the same procedure once more gives Equation X.

$$\frac{d^2y_1}{dx_1^{\,2}} = \frac{1}{K_L} \frac{d^2y_2}{dx_2^{\,2}} \tag{X}$$

Assuming that both full scale and model piles obey the elementary beam equation, the following relationships are valid:

$$\frac{d^2y_1}{dx_1^{\,2}} = \frac{M_1}{E_1I_1} \qquad \frac{d^2y_2}{dx_2^{\,2}} = \frac{M_2}{E_2I_2}$$

If the force scale factor is defined by $K_L = P_1/P_2$, then $M_2 = (1/K_LK_F)M_1$. Substituting into Equation X thus gives

$$\frac{M_1}{E_1I_1} = \frac{1}{K_L}\,\frac{1}{K_LK_F}\,\frac{M_1}{E_2I_2}$$

$$E_2I_2 = \frac{E_1I_1}{K_L^{\,2}K_F} \tag{II}$$

II. Model Pile Section 1

The following quantities are known from full scale data or are chosen arbitrarily:

$$\begin{aligned} E_2I_2 &= 1.404 \times 10^{11} \text{ lb-in}^2 \\ K_L &= 200 \\ t &= 0.5 \text{ in} \\ h &= 0.5 \text{ in} \\ E_1 &= 276{,}000 \text{ psi} \\ L_2 &= 894 \text{ in} \end{aligned}$$

Using the definition of K_L the length of the model Section 1 can be calculated.

$$L_1 = (1/K_L)\ L_2 = 894/200 = 4.47 \text{ in}$$

Using Equation II, the force scale factor, K_F may be determined.

$$K_F = \frac{1}{K_L^{\,2}} \frac{E_2I_2}{E_1I_1} = \frac{1.404\text{x}10^{11}}{(200)^2(2.76\text{x}10^5)(5.21\text{x}10^{-3})} = 2450$$

III. Model Pile Section 2

For Section 2 of the model pile, K_F must be the same as for Section 1, and for convenience the thickness of Section 2 is made the same as Section 1. Thus the following quantities are known:

$$\begin{aligned} E_2I_2 &= 1.100 \times 10^{11} \text{ lb-in}^2 \\ K_L &= 200 \\ K_F &= 2450 \\ L_2 &= 228.5 \text{ in} \\ t &= 0.50 \text{ in} \end{aligned}$$

Using Equation II the height of Section 2 of the pile may be determined.

$$h = \sqrt[3]{\frac{12E_2I_2}{tE_1K_L{}^2K_F}}$$

$$= \sqrt[3]{\frac{12(1.100\text{x}10^{11})}{0.50(2.76\text{x}10^5)(200^2)(2450)}} = 0.460 \text{ in}$$

From the definition of K_L the length of Section 2 may be calculated.

$$L_1 = (1/K_L)\ L_2 = 228.5/200 = 1.143 \text{ in}$$

IV. Model Soil Calculations

Assume the soil modulus increases with depth according to Equation XI.

$$E_s = kT \qquad \text{(XI)}$$

Where T is an increment of depth.

Let E_e = Average modulus over increment T
E_o = Modulus at lower end of increment T
E = Modulus of simulating material
E_T = Modulus at upper end of increment T
t = Thickness of simulating material

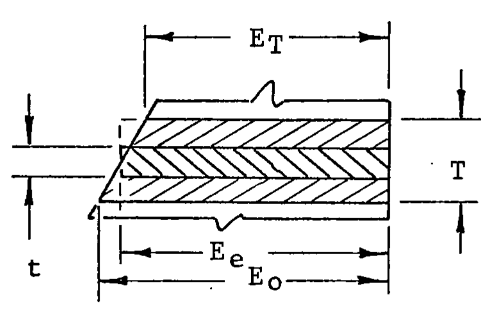

Figure 19
Model Soil Configuration

With the aid of Figure 19, the required lamination thickness, T, can be determined as follows:

$$E_e = 1/2(E_o + E_T)$$
$$E_e = (t/T)E$$
$$E_T = E_o - kT$$

Eliminating E_e and E_T from the equations above yields Equation XII.

$$T = \frac{E_o}{k} - \sqrt{\left(\frac{E_o}{k}\right)^2 - \frac{2tE}{k}} \qquad \text{(XII)}$$

Using Equation XII, the following calculation illustrates the determination of the required thickness, T, for the portion of the model soil immediately above the level having a modulus of 12,000 psi. The material thickness, t, is 0.061 in, the modulus of the plastic, E, is 12,500 psi, and the soil modulus gradient, k, is 6840 psi/in.

$$T = \frac{12,000}{6840} - \sqrt{\left(\frac{12,000}{6840}\right)^2 - \frac{2(0.061)(12,500)}{6840}}$$

$$= 0.070 \text{ in}$$

V. Error Due to Perverted L/D Ratio

The following calculations compare the ratio of shear strain deflection to bending deflection for the model pile and full scale pile in order to illustrate the error due to differences in L/D ratio. The calculations are for the constant shear area between the jack load and top reaction.

The following terms are used in the calculation:

δ_s = Shear deflection
δ_b = Bending deflection
E = Tensile modulus
G = Shear modulus (Poisson's Ratio assumed to be 1/3)
P = Applied load
A = Cross-section area
L = Length between forces
τ = Shear stress
I = Moment of inertia

For the full scale pile:

$$\delta_s = \frac{1}{G}\int_o^L \tau \, dx = \frac{P}{AG}\int_o^L dx = \frac{20,000(27.4)(12)}{\pi(23)(.975)(1.2 \times 10^7)} = .0078 \text{ in}$$

$$\delta_b = \frac{PL^3}{3EI} = \frac{20,000 \; (329)^3}{3(1.4 \times 10^{11})} = 1.69 \text{ in}$$

δ_s = 0.46% of total deflection

For the model pile:

$$\delta_s = \frac{\frac{20,000}{2450} \quad \frac{329}{200}}{(.5)(.5)\frac{267,000}{2.67}} = .000538$$

$$\delta_b = \frac{\frac{20,000}{2450} \quad \left(\frac{329}{200}\right)^3}{3(267,000)(.00521)} = .0087$$

δ_s = 5.85% of total deflection

Thus shear strain is about 10 times more significant in the model than in the full scale pile.